Available online at www.sciencedirect.com
ScienceDirect
Virus Research 122 (2006) 20–27
Virus Research
www.elsevier.com/locate/virusres

Over-expression of severe acute respiratory syndrome coronavirus 3b protein induces both apoptosis and necrosis in Vero E6 cells

Sehaam Khan, Burtram C. Fielding, Timothy H.P. Tan, Chih-Fong Chou, Shuo Shen, Seng Gee Lim, Wanjin Hong, Yee-Joo Tan *

Collaborative Anti-Viral Research Group, Institute of Molecular and Cell Biology, 61 Biopolis Drive, Proteos, Singapore 138673, Singapore

Received 21 March 2006; received in revised form 24 May 2006; accepted 7 June 2006
Available online 11 September 2006

Abstract

The genome of the severe acute respiratory syndrome coronavirus encodes for eight accessory viral proteins with no known homologues in other coronaviruses. One of these is the 3b protein, which is encoded by the second open reading frame in subgenomic RNA 3 and contains 154 amino acids. Here, a detailed time-course study was performed to compare the apoptosis and necrosis profiles induced by full-length 3b, a 3b mutant that was deleted by 30 amino acids from the C terminus (3bΔ124-154) and the classical apoptosis inducer, Bax. Our results showed that Vero E6 cells transfected with a construct for expressing 3b underwent necrosis as early as 6 h after transfection and underwent simultaneous necrosis and apoptosis at later time-points. At all the time-points analysed, the apoptosis induced by the expression of 3b was less than the level induced by Bax but the level of necrosis was comparable. The 3bΔ124-154 mutant behaves in a similar manner indicating that the localization of the 3b protein does not seems to be important for the cell-death pathways since full-length 3b is localized predominantly to the nucleolus, while the mutant is found to be concentrated in the peri-nuclear regions. To our knowledge, this is the first report of the induction of necrosis by a SARS-CoV protein.

Keywords: Coronavirus; SARS coronavirus; Necrosis; Apoptosis; 3b Protein

1. Introduction

Severe acute respiratory syndrome (SARS) originated in early November 2002 in Guangdong province, People's Republic of China. The disease soon spread worldwide infecting more than 8000 people, with more than 700 fatalities (World Health Organization, http://www.who.int/csr/sars/country/en/). The causative agent of SARS was identified as a novel coronavirus, now known as SARS-CoV (for reviews, see Berger et al., 2004; Christian et al., 2004; Peiris et al., 2004). SARS-CoV contains a RNA genome of ∼30 kilobases, which encodes for up to 14 potential open reading frames (ORFs) (Marra et al., 2003; Rota et al., 2003). In addition to the replicase polyproteins (pp1a and pp1ab) and structural proteins, spike, membrane, nucleocapsid and envelope, which are common to all members of the genus coronavirus, the SARS-CoV genome also encodes eight putative proteins with no significant sequence homology to viral proteins of other known coronaviruses (i.e. ORF 3a, 3b, 6, 7a, 7b, 8a, 8b and 9b) (Marra et al., 2003; Snijder et al., 2003; Tan et al., 2005a). It has not yet been established which of the SARS-CoV accessory proteins are essential for viral replication and/or for viral–host interactions. However, the over-expression of some of these SARS-CoV accessory proteins (3a, 7a, 3b) have been shown to induce apoptosis in cell culture (Law et al., 2005; Tan et al., 2004a; Yuan et al., 2005a), suggesting that they may play a role in viral pathogenesis.

The second largest subgenomic RNA of SARS-CoV (sgRNA3) contains two ORFs, 3a and 3b. The 3a protein has been characterized to a great extent and has been shown to be expressed in infected cells both in vitro and in vivo (Chan et al., 2005; Ito et al., 2005; Law et al., 2005; Tan et al., 2004c; Yu et al., 2004; Zeng et al., 2004). It is a novel coronavirus structural protein (Ito et al., 2005; Shen et al., 2005) and can up-regulate the expression of fibrinogen in lung cells (Tan et al., 2005b). The 3b protein is likely to be expressed via an internal ribosomal entry mechanism since its translation initiation codon is not the first AUG in sgRNA3 (Snijder et al., 2003). It has been detected in SARS-CoV infected cells (Chan et al., 2005), and

* Corresponding author. Tel.: +65 65869625; fax: +65 67791117.
E-mail address: mcbtanyj@imcb.a-star.edu.sg (Y.-J. Tan).

0168-1702/$ – see front matter © 2006 Elsevier B.V. All rights reserved.
doi:10.1016/j.virusres.2006.06.005

anti-3b antibody has been detected in a SARS patient's serum (Guo et al., 2004), suggesting that it is expressed in vivo. The 3b protein contains two predicted nuclear localization signals and has been shown to localize to the nucleolus of transfected cells in the absence of any other SARS-CoV proteins (Yuan et al., 2005b). In addition, the over-expression of 3b causes G0/G1 arrest and induces apoptosis (Yuan et al., 2005a).

In this study, we determined the mechanism of cell-death induced by the over-expression of full-length 3b or a 3b mutant that lacks the C-terminal 30 amino acids (3bΔ124-154). By following the time-course of expression, we compared the apoptosis and necrosis profiles induced by full-length 3b, 3bΔ124-154 mutant and the classical apoptosis inducer, Bax. Terminal deoxynucleotidyl transferase mediated dUTP nick-end-labeling (TUNEL) assays and subcellular fractionation were performed to further delineate the cell-death pathways.

2. Methods

2.1. Materials

All reagents used in this study were purchased from Sigma (St. Louis, MO, USA) unless otherwise stated. Vero E6 (African green monkey kidney epithelial) cells were grown in Dulbecco's modified Eagle medium containing 0.1 mg/ml streptomycin and 100 U penicillin and 5% FBS (HyClone, UT, USA). Cells were cultured at 37 °C in an incubator supplied with 5% CO_2.

2.2. Construction of plasmids

To clone the 3b gene into pXJ40HA mammalian expression vector, the 3b ORF was amplified using 3b-forward (5′-CCGCTCGAGGCCACCATGATGCCAA-3′) and 3b-reverse (5′-ATAAGAATGCGGCCGCTTAACGTACCTGTTTC-3′) primers. cDNA prepared from SARS-CoV infected cells was used as template as previously described (Tan et al., 2004b). The PCR product was digested with restriction enzymes (*Xho*I and *Not*I) and ligated to linearized pXJ40HA digested with the same restriction enzymes. The pXJ40HA-3bΔ124-154 plasmid for expressing a 3b mutant without the C-terminal 30 amino acids was made in a similar manner using the 3b-forward primer and 3bΔ124-154-reverse (5′-ATAAGAATGCGGCCGCTTACATCATAAATTG-3′) primer. All plasmid sequences were confirmed by sequence analysis.

2.3. Transfection and CaspACE fluorometric assay

Vero E6 cells were plated on 6 cm tissue culture dishes and allowed to grow to 70% confluence before the cells were transfected with 3 μg of pXJ40HA-3b or pXJ40HA-3bΔ124-154 using Lipofectamine reagent (Invitrogen, Carlsbad, CA), according to manufacturer's protocol. To reduce the rate of apoptosis induced by the potent apoptosis inducer, Bax, 1 μg of pXJ40HA-Bax was used with 2 μg of empty vector instead. For mock transfection, no DNA was used but the cells were incubated with the same amount of Lipofectamine reagent.

Each plate of cells was harvested at various time-points, i.e. 6, 12, 18 and 48 h, after transfection. The cells were then washed with phosphate-buffered saline (PBS) and resuspended in 110 μl of lysis buffer (50 mM Tris–HCl (pH 8.0), 150 mM NaCl, 0.5% NP40, 0.5% deoxycholic acid, 0.005% SDS), containing 1 mM PMSF. Half of the suspension was then subjected to three rounds of freeze-thaw cycles and then centrifuged to remove cell debris. The total protein concentration of the lysate was determined by using Coomassie Plus reagent from Pierce (Rockford, IL). The amount of caspase-3 activity in 10 μg of total protein was then determined by using the CaspACE fluorometric assay system from Promega Corporation (Madison, WI). All experiments were performed in duplicates. Laemmli's sodium dodecyl sulphate buffer (SDS buffer) was added to the other half of the cell suspension. As the 3b protein tends to form large aggregates when boiled, the SDS–cell mixture was incubated at 50 °C for 15 min before Western blot analysis. For HA-Bax, the SDS–cell mixture was heated at 100 °C for 10 min.

2.4. Western blot analysis

For Western blot analysis, cell lysates were separated on SDS-PAGE and transferred onto Hybond-C membranes (Amersham Pharmacia Biotech, Uppsala, Sweden). The membranes were then blocked with 5% non-fat milk for 30 min and probed with primary antibodies (anti-HA monoclonal antibody (1:1000; Roche Molecular Biochemicals, Indianapolis, IN) or anti-poly(ADP-ribose) polymerase (PARP) polyclonal antibody (1:1000; Cell Signaling Technology, Inc., Beverly, MA) or anti-actin monoclonal antibody (1:3000; Sigma)) with rolling at 4 °C overnight. After three washes (15 min each) with PBS containing 0.05% Tween 20 (PBST), the membranes were incubated with goat anti-rabbit or anti-mouse horse-radish peroxidase (HRP)-conjugated secondary antibodies (1:2000, Pierce) at room temperature, with rolling for 1 h. The membranes were then washed with PBST three times for 15 min each, and visualized using an enhanced chemiluminescence method (Supersignal West Pico, Pierce).

2.5. CytoTox-ONE homogenous membrane integrity assay

Vero E6 cells were plated in 6 cm tissue culture dish and transfected as described above. At each time-point, 110 μl of the culture medium were transferred to a 96-well plate and the amount of lactate dehydrogenase (LDH) released from damaged necrotic cells was determined using the CytoTox-ONE homogenous membrane integrity assay (Promega) according to manufacturer's protocol. All experiments were performed in duplicates.

2.6. DeadENd fluorometric TUNEL and immunofluorescence experiments

Vero E6 cells were seeded on cover slips and transfected as described above. Cells were analysed for DNA fragmentation by using the DeadENd fluorometric TUNEL system (Promega) according to manufacturer's protocol. Cells treated with DNase

I (Roche) served as a positive control. The cell nuclei were counterstained with 1 μg/ml propidium iodide.

For immunofluorescence experiments, the cover slips were fixed in methanol for 5 min at −20 °C, after which the cover slips were completely air-dried. Cells were blocked with PBS with 1% bovine serum albumin for 30 min, and then incubated with anti-HA antibody at a dilution of 1:200 for 1 h. Following washing, cells were incubated with the fluorescein isothicyanate (FITC)-conjugated goat anti-mouse secondary antibody (1:100; Santa Cruz Biotechnology, Santa Cruz, CA) for 1 h.

2.7. Subcellular fractionation

Vero E6 cells were plated in 10 cm tissue culture dish and transfected as described above. In this case, 6 μg of pXJ40HA-3b or pXJ40HA-3bΔ124-154 was used. Fractionation was then performed to separate the cytoplasmic, nuclear and membrane components of the cell. The method used was adapted from Spector et al. (1988) with some modifications and is described below.

At different time-points, the cells were harvested and washed twice with cold PBS and resuspended in 200 μl hypotonic buffer (10 mM Tris–HCl (pH 7.5), 2 mM $MgCl_2$, 0.5 mM PMSF) and left in ice-water for 5 min. 0.25% Triton-X 100 was then added and the cells were sheared by passing through a 21G needle thrice. The cells was then left in ice-water for 5 min and spun at 3000 rpm at 4 °C for 5 min (step A). The supernatant was transferred to a clean tube and spun again at 14,000 rpm at 4 °C for 20 min (step B) and the supernatant was collected (cytoplasmic fraction). The pellet after step B (membrane fraction) was resuspended in 200 μl of lysis buffer with DNase I (1 μl/ml), and left at room temperature for 15 min to degrade the cellular DNA. To wash the pellet from step A (nuclear fraction), it was resuspended in 0.5 ml ice-cold hypotonic buffer and spun at 3000 rpm at 4 °C for 5 min and the supernatant was discarded. After two washes, the pellet was resuspended in 200 μl of lysis buffer with DNase I. Finally, 50 μl of 5XSDS buffer was added to each of the fractions and the mixtures were vortexed and left at room temperature for 15 min, followed by incubation at 50 °C for 15 min. Then, 20 μl of each fraction was subjected to Western blot analysis as described above.

3. Results and discussion

Recently, Yuan and co-workers showed that the over-expression of SARS-CoV 3b in COS-7, Vero and 293 induces cell-cycle arrest but they could only observed significant apoptosis in COS-7 cells (Yuan et al., 2005a). Here, a time-course study was performed to characterize the profile of cell-death induced by the over-expression of 3b in Vero E6 cells in order to understand the role of 3b during the viral replication cycle in Vero E6 cells. In addition, the cell-death profiles of full-length 3b and a deletion mutant, 3bΔ124-154, which lacks the C-terminal 30 amino acids, were compared to that of Bax, a classical apoptosis inducer. The general opinion is that cell death can either be as a result of necrosis, defined as a passive and non-physiological type of death caused by accidental and acute damage to the cell, or the consequence of apoptosis, defined as an active and genetically regulated process of cell suicide by which an organism eliminates senescent, abnormal and potentially harmful cells (for reviews, see Ameison, 2002; Guimarães and Linden, 2004; Los et al., 2002; Nelson and White, 2004; Zhivotosky, 2004). These two forms of cell death are distinguishable by their morphological and biochemical effects on the cell. However, recent studies have shown that necrosis is also highly regulated and a fine regulatory line exists between necrosis and apoptosis as many anti-apoptotic mechanisms are also effective against necrosis (for reviews, see Proskuryakov et al., 2003; Syntichaki and Tavernarakis, 2002, 2003). For the sake of simplicity, we shall use the term necrosis to refer to the form of cell death not involving the apoptotic early steps, and secondary necrosis to describe the subsequent degradative changes that apoptotic cells undergo at the late stages of apoptosis.

Vero E6 cells were analysed at 6, 12, 18 and 48 h after transfection with plasmids for expressing HA-3b, HA-3bΔ124-154 and HA-Bax to determine the degree of apoptosis and necrosis. The expression of the proteins were detected using anti-HA monoclonal antibody (Fig. 1A and B). As shown in Fig. 1C, the over-expression of 3b and 3bΔ124-154 resulted in a slight increase in caspase 3 activity, which is a hallmark of apoptosis, at 6 h post-transfection. The level of caspase 3 activity continued to increase until 12 h after transfection but showed gradual decrease at 18 and 48 h after transfection. Consistently, the expression of 3b and 3bΔ124-154 also resulted in cleavage of endogenous PARP, which is a substrate of activated caspase-3 (Fig. 1A) from 12 h onwards. This profile mirrored that of Bax, except that the level of caspase 3 activities for 3b and 3bΔ124-154 were lower than for Bax at all the time-points and that Bax already showed high level of caspase 3 activities and PARP cleavage at 6 h (Fig. 1B and C). These results are somewhat different from the report by Yuan et al. (2005a) where the over-expression of 3b did not induce apoptosis in Vero cells, and furthermore, showed that the C-terminal 30 amino-acids of 3b are not important for apoptosis induction. The discrepancy may be due to differences in transfection efficiency and/or sensitivity of the assays used.

In all cases, we noted that a decease in caspase 3 activity after 18 h of transfection, suggesting that the apoptotic cells were going into secondary necrosis. A key marker of a cell undergoing necrosis is the loss of their membrane integrity and the release of their cytoplasmic contents into the surrounding culture. Thus, the CytoTox-ONE assay (Promega), which measures the release of lactate dehydrogenase (LDH) from cells with damaged membranes, was used to quantify the degree of necrosis at different time-points. For the over-expression of 3b and 3bΔ124-154, significant amounts of LDH were released as early as 6 h post-transfection as compared to the low level of LDH released from mock transfected cells (Fig. 1D). The levels of LDH then increased gradually up to 12 h. Interestingly, the level of LDH released from cells expressing Bax was about the same as for 3b and 3bΔ124-154 at 6 h, 12 h and 18 h, even though the level of apoptosis caused by the over-expression of Bax was consistently higher that caused by 3b or 3bΔ124-154. The gradual increase in the level of necrosis in the Bax expressing cells was expected as apoptotic cells would undergo secondary necrosis

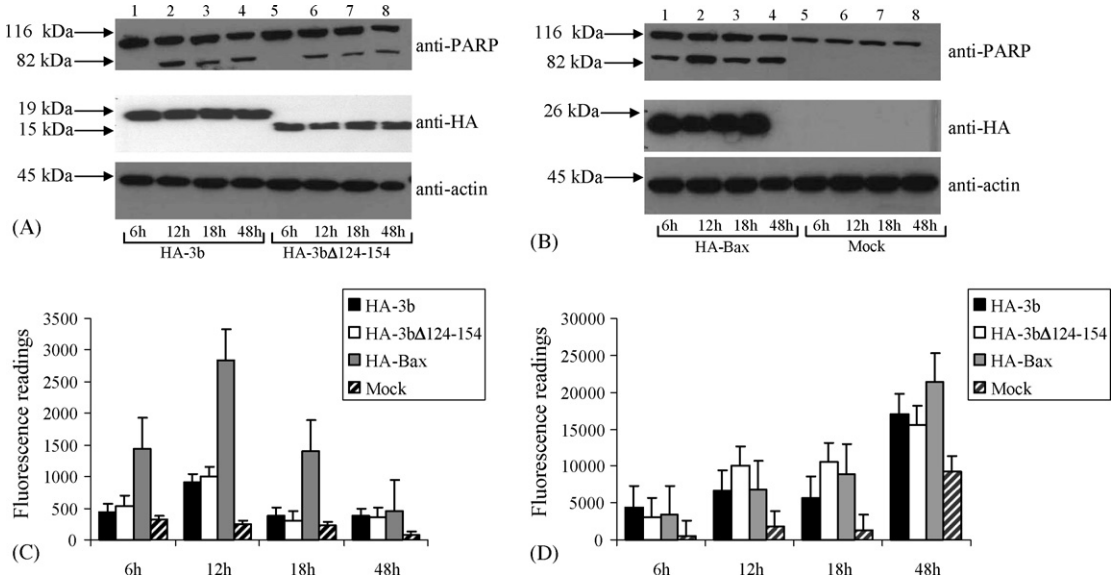

Fig. 1. Time-course study to determine the effects of the expression of SARS-CoV 3b proteins on apoptosis and necrosis. (A and B) Western blot analysis was performed to determine the expression of full-length SARS-CoV 3b ((A), lanes 1–4)), a 3b mutant which lacks the C-terminal 30 amino acids (3bΔ124-154) ((A), lanes 5–8) and Bax ((B), lanes 1–4), a potent apoptosis inducer in transiently transfected Vero E6 cells. All proteins were tagged at the N-terminal with a HA motif for easy detection. Cells were harvested at 6, 12, 18 and 48 h post-transfection and the expression levels of HA-tagged proteins were determined with anti-HA antibody (middle panel). Mock transfected cells were used as negative control. The same samples were assayed for the cleavage of endogenous full-length PARP, which is a hallmark of apoptosis, from 116 to 83 kDa (upper panel). Equal loading of total cell lysates were verified by using an antibody to detect endogenous actin (lower panel). (C) The CaspACE fluorometric assay system from Promega Corporation was used to measure the activation of caspase-3 protease activity, which is another hallmark of apoptosis. (D) The CytoTox-ONE homogenous membrane integrity assay from Promega Corporation was used to measure the amount of lactate dehydrogenase (LDH) released from necrotic cells. For (C and D), these assays were performed at each time-point for HA-3b (solid black bars), HA-3bΔ124-154 (unshaded bars), HA-Bax (solid gray bars) and mock transfected cells (striated bars). All experiments were performed in duplicates and the average values with standard deviations are plotted.

at the late stages (Ameison, 2002; Guimarães and Linden, 2004; Los et al., 2002; Nelson and White, 2004; Zhivotosky, 2004). These results showed that the expression of 3b induces necrosis as early as 6 h post-transfection when the level of apoptosis was very much lower than that for Bax. Again, the C-terminal 30 amino acids of 3b do not have any effects on its ability to induce necrosis. At time-points greater than 6 h post-infection, it appears that both necrosis and apoptosis (and secondary necrosis) were occurring simultaneously in cell over-expressing 3b or 3bΔ124-154. At 48 h post-transfection, there was a surge of LDH release from cells expressing 3b or 3bΔ124-154 or Bax or even the mock transfected cells, indicating that by this time, the Lipofectamine reagent used for transfection had some unspecific cytotoxic effects or the cells were over-grown (Fig. 1D). Thus, subsequent experiments were only performed up to 18 h post-transfection.

TUNEL assays were performed to examine whether the 3b and 3bΔ124-154 could induce DNA fragmentation, a common phenomenon of apoptosis. At all the time-points, DNA fragmentations were observed in 3b- and 3bΔ124-154-transfected Vero E6 cells. A representative set of data for 18 h post-transfection is shown in Fig. 2 (first and second rows). DNA fragmentations in cells expressing 3b or 3bΔ124-154 (note that the typical transfection efficiency achieved in this study was about 30%) were indicated by FITC positive signals while nuclei of all the cells in the field were counterstained using propidium iodide. DNA fragmentation was also be detected in the cells transfected with Bax (Fig. 2, third row) and in cells that were treated with DNase I (positive control) (Fig. 2, fifth row). Under the same exposure conditions, there was no sign of DNA fragmentation in the mock transfected cells (Fig. 2, fourth row).

Next, the subcellular localization of 3b and 3bΔ124-154 was examined by subcellular fractionation studies performed at 6, 12 and 18 h post-transfection. Consistent with previous report (Yuan et al., 2005b), the full-length 3b protein was found to partition solely in the nuclear fraction at all the time-points (Fig. 3A). The 3b deletion mutant, 3bΔ124-154, was initially found in the cytoplasmic fraction (6 h post-transfection), but with time, could be more efficiently detected in the membrane and nuclear fractions (Fig. 3B). As a control for the fractionation method, endogenous actin was detected in the cytoplasmic fractions for all transfections.

Next, indirect immunofluorescence was also performed at 18 h post-transfection to compare the subcellular localization of 3b and 3bΔ124-154 in Vero E6 cells (Fig. 3C). Consistent with the fractionation experiments above, indirect immunofluorescence revealed that the 3b protein was localized primarily in the nucleolus of transfected cells and somewhat less around the nucleus. The latter is likely to be the nuclear membrane as 3b was isolated in the nuclear fraction (Fig. 3A). In contrast, 3bΔ124-154 was localized to the perinuclear regions, while Bax was diffusely localized in the cytoplasm. Since the fractionation experiments showed that 3bΔ124-154 was found predominantly in the membrane and nuclear fractions at late

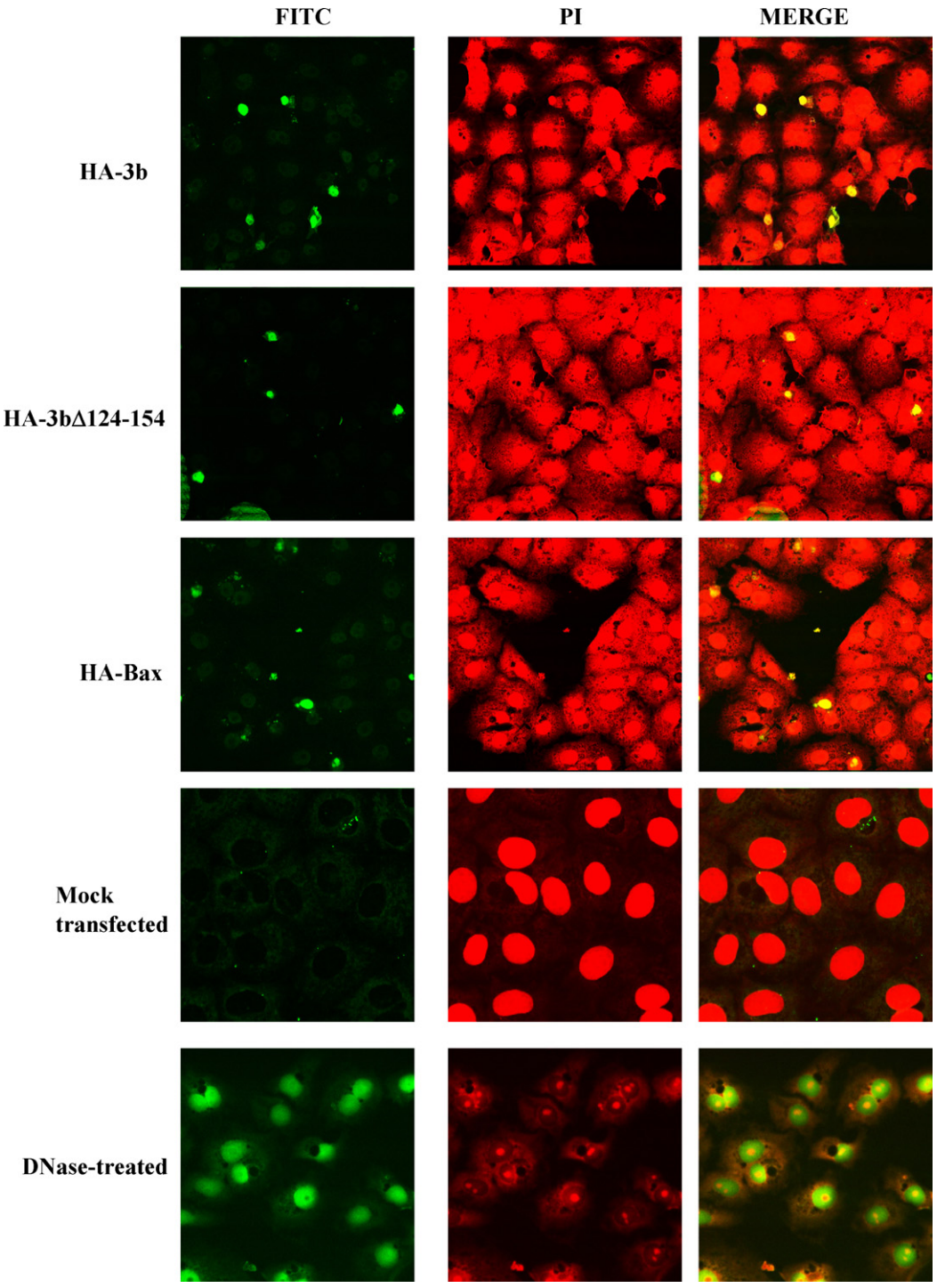

Fig. 2. DNA fragmentation in Vero E6 cells expressing HA-3b, HA-3bΔ124-154 and HA-Bax, detected by TUNEL assay. Fragmented DNA showed FITC (green, left panels) staining in the nucleus while the nuclei of all the cells in the same field were counterstained with propidium iodide (PI, red, middle panels). The right panels showed the merged image of FITC and PI staining and cells containing fragmented DNA would have a yellow colour. The positive control was DNase I treated cells and negative control was mock transfected cells.

time-points (Fig. 3B), it is likely that the intense staining around the nucleus represents both perinuclear membranous organelles, like the endoplasmic reticulum or Golgi apparatus, as well as nuclear membrane, with the latter being partitioned into the nuclear fraction. Amino acids 134–154 of 3b have been previously shown to contain a nucleolar localization signal (Yuan et al., 2005b). Consistently, we observed that unlike full-length 3b, the 3bΔ124-154 mutant was not efficiently transported to the nucleolus.

In summary, we demonstrated that Vero E6 cells transfected with a construct for expressing 3b underwent necrosis as early as 6 h after transfection and underwent simultaneous necrosis and apoptosis at later time-points. At all the time-points analysed, the apoptosis induced by the expression of 3b was less than the

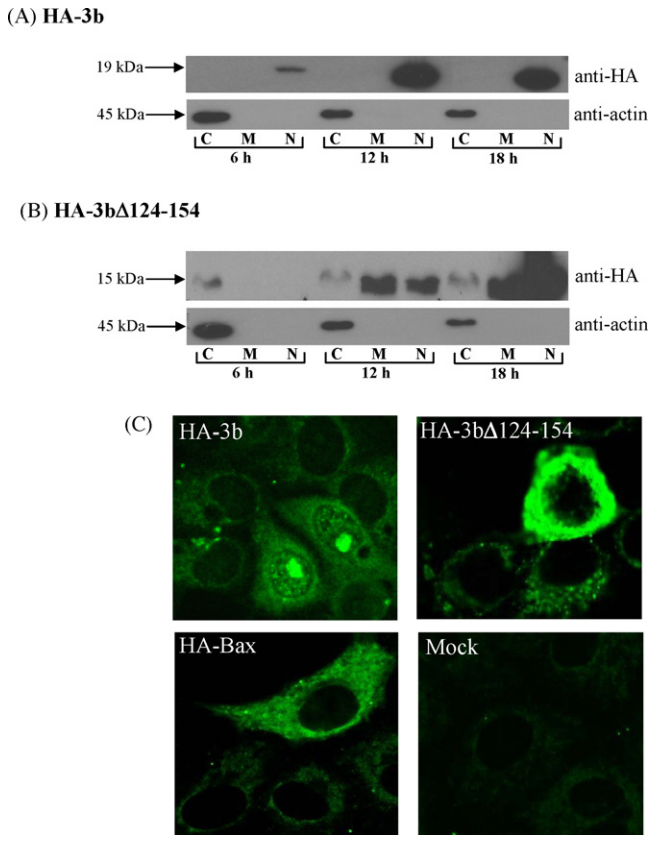

Fig. 3. Cellular localization of HA-3b and HA-3bΔ124-154 proteins. Subcellular fractionation was performed to separate the cells into cytoplasmic (C), membrane (M) and nuclear (N) fractions. Western analyses were performed using with anti-HA (upper panel) and anti-actin (lower panel) monoclonal antibodies for each protein: (A) HA-3b; (B) HA-3bΔ124-154. The migration of protein molecular weight markers is indicated on the left. (C) The cellular localization of HA-3b, HA-3bΔ124-154, HA-Bax were analysed by indirect immunofluorescence at 18 h post-transfection. Mock transfected cells showed the specificity of the anti-HA monoclonal antibody.

level induced by Bax but the level of necrosis was comparable to that induced by over-expression of Bax. Hence, it is clear that 3b induces necrosis at the early time-point and apoptosis (and secondary necrosis) at late time-points. The deletion mutant 3bΔ124-154 behaves in a similar manner indicating that the localization of 3b does not seems to be important for the cell-death pathways since full-length 3b is localized predominantly to the nucleolus, while the mutant is found to be concentrated in the peri-nuclear regions.

Recently, Yount et al. (2005) showed by reverse genetics experiment that recombinant virus containing a deletion of the ORF3a, which resulted in the movement of ORF3b to the 5′ end of the mRNA and an increase in the level of 3b expression, has a lower viral yield than wild-type virus. On the other hand, if both 3a and 3b are deleted, there is no significant difference from wild-type virus, thus suggesting that the over-expression of 3b may have a deleterious effect on viral yield (Yount et al., 2005). It remains to be determined if the necrotic effect on the cells caused by the over-expression of 3b could play a part in reducing the viral titre. Interestingly, Hussain et al. (2005) reported that the 3b protein can also be expressed from an independent subgenomic RNA but this is a rare event. Given the findings that over-expression of 3b can cause rapid necrosis and may reduce virus titer in cell culture systems, it is crucial to further understand how the expression level of 3b is modulated during SARS-CoV infection.

Many virus genomes encode gene products that can modulate apoptosis and the regulation of apoptosis in infected the host is an important determinant in the struggle between virus and host for survival (for review, see Barber, 2001; Benedict et al., 2002; Boya et al., 2001; Hay and Kannourakis, 2002; Mori et al., 2004; Thomson, 2001). However, the role of necrosis in viral infection is less clear, partly because the necrosis process is less well-studied. Nevertheless, to date, necrosis has been shown to play an important role during viral infection by at least four viruses (An et al., 2000; Espinoza et al., 2005; Miller and Fox, 2004; Ran et al., 1999). Whether or not necrosis is important for SARS-CoV infection remains to be determined. Interestingly, necrosis was observed in different tissues obtained from SARS-CoV infected patients (Chong et al., 2004; Ding et al., 2003; Lang et al., 2003; Xu et al., 2005) and many SARS-CoV infected laboratory animals, including cynomologus macaques (Fouchier et al., 2003; Kuiken et al., 2003), rhesus macaques (Qin et al., 2005), common marmosets (Greenough et al., 2005), golden syrian hamster (Roberts et al., 2005b) and aged BALB/c mice (Roberts et al., 2005a). However, necrosis was not observed in SARS-CoV infected Vero E6 cells (Yan et al., 2004), suggesting that the level of 3b may not be sufficient to induce necrosis in Vero E6 cells. However, we cannot rule out that the expression of 3b may be higher in SARS patients and/or SARS-CoV infected animals than in SARS-CoV infected cell culture. Further studies using animal models will be necessary to give a more definitive answer.

Acknowledgement

This work was supported by grants from the Agency for Science, Technology and Research (A*STAR), Singapore.

References

Ameison, J.C., 2002. On the origin, evolution, and nature of programmed cell death: a timeline of four billion years. Cell Death Differ. 9, 367–393.

An, K., Fattaey, H.K., Paulsen, A.Q., Consigli, R.A., 2000. Murine polyomavirus infection of 3T6 mouse cells shows evidence of predominant necrosis as well as limited apoptosis. Virus Res. 67, 81–90.

Barber, G.N., 2001. Host defense, viruses and apoptosis. Cell Death Differ. 8, 113–126.

Benedict, C.A., Norris, P.S., Ware, C.F., 2002. To kill or be killed: viral evasion of apoptosis. Nat. Immunol. 3, 1013–1018.

Berger, A., Drosten, Ch., Doerr, H.W., Sturmer, M., Preiser, W., 2004. Severe acute respiratory syndrome (SARS)—paradigm of an emerging viral infection. J. Clin. Virol. 29, 13–22.

Boya, P., Roques, B., Kroemer, G., 2001. Viral and bacterial proteins regulating apoptosis at the mitochondrial level. EMBO J. 20, 4325–4331.

Chan, W.S., Wu, C., Chow, S.C., Cheung, T., To, K.F., Leung, W.K., Chan, P.K., Lee, K.C., Ng, H.K., Au, D.M., Lo, A.W., 2005. Coronaviral hypothetical and structural proteins were found in the intestinal surface enterocytes and pneumocytes of severe acute respiratory syndrome (SARS). Mod. Pathol. 18, 1432–1439.

Chong, P.Y., Chui, P., Ling, A.E., Franks, T.J., Tai, D.Y., Leo, Y.S., Kaw, G.J., Wansaicheong, G., Chan, K.P., Ean Oon, L.L., Teo, E.S., Tan, K.B., Nakajima, N., Sata, T., Travis, W.D., 2004. Analysis of deaths during the severe acute respiratory syndrome (SARS) epidemic in Singapore: challenges in determining a SARS diagnosis. Arch. Pathol. Lab. Med. 128, 195–204.

Christian, M.D., Poutanen, S.M., Loutfy, M.R., Muller, M.P., Low, D.E., 2004. Severe acute respiratory syndrome. Clin. Infect. Dis. 38, 1420–1427.

Ding, Y., Wang, H., Shen, H., Li, Z., Geng, J., Han, H., Cai, J., Li, X., Kang, W., Weng, D., Lu, Y., Wu, D., He, L., Yao, K., 2003. The clinical pathology of severe acute respiratory syndrome (SARS): a report from China. J. Pathol. 200, 282–289.

Espinoza, J.C., Cortes-Gutierrez, M., Kuznar, J., 2005. Necrosis of infectious pancreatic necrosis virus (IPNV) infected cells rarely is preceded by apoptosis. Virus Res. 109, 133–138.

Fouchier, R.A., Kuiken, T., Schutten, M., van Amerongen, G., van Doornum, G.J., van den Hoogen, B.G., Peiris, M., Lim, W., Stohr, K., Osterhaus, A.D., 2003. Aetiology: Koch's postulates fulfilled for SARS virus. Nature 423, 240.

Greenough, T.C., Carville, A., Coderre, J., Somasundaran, M., Sullivan, J.L., Luzuriaga, K., Mansfield, K., 2005. Pneumonitis and multi-organ system disease in common marmosets (Callithrix jacchus) infected with the severe acute respiratory syndrome-associated coronavirus. Am. J. Pathol. 167, 455–463.

Guimarães, C.A., Linden, R., 2004. Programmed cell death: apoptosis and alternative deathstyles. Eur. J. Biochem. 271, 1638–1650.

Guo, J.P., Petric, M., Campbell, W., McGeer, P.L., 2004. SARS corona virus peptides recognized by antibodies in the sera of convalescent cases. Virology 324, 251–256.

Hay, S., Kannourakis, G., 2002. A time to kill: viral manipulation of the cell death program. J. Gen. Virol. 83, 1547–1564.

Hussain, S., Pan, J., Chen, Y., Yang, Y., Xu, J., Peng, Y., Wu, Y., Li, Z., Zhu, Y., Tien, P., Guo, D., 2005. Identification of novel subgenomic RNA's and noncanonical transcription initiation siganals of severe acute respiratory syndrome coronavirus. J. Virol. 79, 5288–5295.

Ito, N., Mossel, E.C., Narayanan, K., Popov, V.L., Huang, C., Inoue, T., Peters, C.J., Makino, S., 2005. Severe acute respiratory syndrome coronavirus 3a protein is a viral structural protein. J. Virol. 79, 3182–3186.

Kuiken, T., Fouchier, R.A., Schutten, M., Rimmelzwaan, G.F., van Amerongen, G., van Riel, D., Laman, J.D., de Jong, T., van Doornum, G., Lim, W., Ling, A.E., Chan, P.K., Tam, J.S., Zambon, M.C., Gopal, R., Drosten, C., van der Werf, S., Escriou, N., Manuguerra, J.C., Stohr, K., Peiris, J.S., Osterhaus, A.D., 2003. Newly discovered coronavirus as the primary cause of severe acute respiratory syndrome. Lancet 362, 263–270.

Lang, Z.W., Zhang, L.J., Zhang, S.J., Meng, X., Li, J.Q., Song, C.Z., Sun, L., Zhou, Y.S., Dwyer, D.E., 2003. A clinicopathological study of three cases of severe acute respiratory syndrome (SARS). Pathology 35, 526–531.

Law, P.T., Wong, C.H., Au, T.C., Chuck, C.P., Kong, S.K., Chan, P.K., To, K.F., Lo, A.W., Chan, J.Y., Suen, Y.K., Chan, H.Y., Fung, K.P., Waye, M.M., Sung, J.J., Lo, Y.M., Tsui, S.K., 2005. The 3a protein of severe acute respiratory syndrome-associated coronavirus induces apoptosis in Vero E6 cells. J. Gen. Virol. 86, 1921–1930.

Los, M., Mozoluk, M., Ferrari, D., Stepczynska, A., Stroh, C., Renz, A., Herceg, Z., Wang, Z.-Q., Schulze-Osthoff, K., 2002. Activation and caspase-mediated inhibition of PARP: A molecular switch between fibroblast necrosis and apoptosis in death receptor signalling. Mol. Biol. Cell. 13, 978–988.

Marra, M.A., Jones, S.J., Astell, C.R., Holt, R.A., Brooks-Wilson, A., Butterfield, Y.S., Khattra, J., Asano, J.K., Barber, S.A., Chan, S.Y., Cloutier, A., Coughlin, S.M., Freeman, D., Girn, N., Griffith, O.L., Leach, S.R., Mayo, M., McDonald, H., Montgomery, S.B., Pandoh, P.K., Petrescu, A.S., Robertson, A.G., Schein, J.E., Siddiqui, A., Smailus, D.E., Stott, J.M., Yang, G.S., Plummer, F., Andonov, A., Artsob, H., Bastien, N., Bernard, K., Booth, T.F., Bowness, D., Czub, M., Drebot, M., Fernando, L., Flick, R., Garbutt, M., Gray, M., Grolla, A., Jones, S., Feldmann, H., Meyers, A., Kabani, A., Li, Y., Normand, S., Stroher, U., Tipples, G.A., Tyler, S., Vogrig, R., Ward, D., Watson, B., Brunham, R.C., Krajden, M., Petric, M., Skowronski, D.M., Upton, C., Roper, R.L., 2003. The Genome sequence of the SARS-associated coronavirus. Science 300, 1399–1404.

Miller, L.C., Fox, J.M., 2004. Apoptosis and porcine reproductive and respiratory syndrome virus. Vet Immunol. Immunopathol. 102, 131–142.

Mori, I., Nishiyama, Y., Yokochi, T., Kimura, Y., 2004. Virus-induced neuronal apoptosis as pathological and protective responses of the host. Rev. Med. Virol. 14, 209–216.

Nelson, D.A., White, E., 2004. Exploiting different ways to die. Genes Dev. 18, 1223–1226.

Peiris, J.S., Guan, Y., Yuen, K.Y., 2004. Severe acute respiratory syndrome. Nat. Med. 10 (Suppl.), S88–S97.

Proskuryakov, S.Y., Konoplyannikov, A.G., Gabai, V.L., 2003. Necrosis: a specific form of programmed cell death? Exp. Cell Res. 283, 1–16.

Qin, C., Wang, J., Wei, Q., She, M., Marasco, W.A., Jiang, H., Tu, X., Zhu, H., Ren, L., Gao, H., Guo, L., Huang, L., Yang, R., Cong, Z., Guo, L., Wang, Y., Liu, Y., Sun, Y., Duan, S., Qu, J., Chen, L., Tong, W., Ruan, L., Liu, P., Zhang, H., Zhang, J., Zhang, H., Liu, D., Liu, Q., Hong, T., He, W., 2005. An animal model of SARS produced by infection of Macaca mulatta with SARS coronavirus. J. Pathol. 206, 251–259.

Ran, Z., Rayet, B., Rommelaere, J., Faisst, S., 1999. Parvovirus H-1-induced cell death: influence of intracellular NAD consumption on the regulation of necrosis and apoptosis. Virus Res. 65, 161–174.

Roberts, A., Paddock, C., Vogel, L., Butler, E., Zaki, S., Subbarao, K., 2005a. Aged BALB/c mice as a model for increased severity of severe acute respiratory syndrome in elderly humans. J. Virol. 79, 5833–5838.

Roberts, A., Vogel, L., Guarner, J., Hayes, N., Murphy, B., Zaki, S., Subbarao, K., 2005b. Severe acute respiratory syndrome coronavirus infection of golden Syrian hamsters. J. Virol. 79, 503–511.

Rota, P.A., Oberste, M.S., Monroe, S.S., Nix, W.A., Campagnoli, R., Icenogle, J.P., Penaranda, S., Bankamp, B., Maher, K., Chen, M.H., Tong, S., Tamin, A., Lowe, L., Frace, M., DeRisi, J.L., Chen, Q., Wang, D., Erdman, D.D., Peret, T.C., Burns, C., Ksiazek, T.G., Rollin, P.E., Sanchez, A., Liffick, S., Holloway, B., Limor, J., McCaustland, K., Olsen-Rasmussen, M., Fouchier, R., Gunther, S., Osterhaus, A.D., Drosten, C., Pallansch, M.A., Anderson, L.J., Bellini, W.J., 2003. Characterization of a novel coronavirus associated with severe acute respiratory syndrome. Science 300, 1394–1399.

Shen, S., Lin, P.S., Chao, Y.-C., Zhang, A., Yang, X., Lim, S.G., Hong, W., Tan, Y.-J., 2005. The severe acute respiratory syndrome coronavirus 3a is a novel structural protein. Biochem. Biophys. Res. Commun. 330, 286–292.

Snijder, E.J., Bredenbeek, P.J., Dobbe, J.C., Thiel, V., Ziebuhr, J., Poon, L.L., Guan, Y., Rozanov, M., Spaan, W.J., Gorbalenya, A.E., 2003. Unique and conserved features of genome and proteome of SARS-coronavirus, an early split-off from the coronavirus group 2 lineage. J. Mol. Biol. 331, 991–1004.

Spector, D.L., Goldman, R.D., Leinwand, L.A., 1988. Cells, a laboratory manual. Culture and Biochemical Analysis of Cells, vol. 1. Cold Spring Harbor Laboratory Press, USA.

Syntichaki, P., Tavernarakis, N., 2002. Death by necrosis. Uncontrollable catastrophe, or is there order behind the chaos? EMBO Rep. 3, 604–609.

Syntichaki, P., Tavernarakis, N., 2003. The biochemistry of neuronal necrosis: rogue biology? Nat. Rev. Neurosci. 4, 672–684.

Tan, Y.J., Fielding, B.C., Goh, P.Y., Shen, S., Tan, T.H.P., Lim, S.G., Hong, W., 2004a. Overexpression of 7a, a protein specifically encoded by the severe acute respiratory syndrome coronavirus, induces apoptosis via a caspase-dependent pathway. J. Virol. 78, 14043–14047.

Tan, Y.-J., Goh, P.-Y., Fielding, B.C., Shen, S., Chou, C.-F., Fu, J.-L., Leong, H.N., Leo, Y.S., Ooi, E.E., Ling, A.E., Lim, S.G., Hong, W., 2004b. Profile of antibody responses against SARS-Coronavirus recombinant proteins and their potential use as diagnostic markers. Clin. Diag. Lab. Immunol. 11, 362–371.

Tan, Y.-J., Teng, E., Shen, S., Tan, T.H.P., Goh, P.-Y., Fielding, B.C., Ooi, E.-E., Tan, H.-C., Lim, S.G., Hong, W., 2004c. A novel SARS coronavirus protein, U274, is transported to the cell surface and undergoes endocytosis. J. Virol. 78, 6723–6734.

Tan, Y.-J., Lim, S.G., Hong, W., 2005a. Characterization of viral proteins encoded by the SARS-coronavirus genome. Antiviral Res. 65, 69–78.

Tan, Y.-J., Tham, P.Y., Chan, D.Z., Chou, C.F., Shen, S., Fielding, B.C., Tan, T.H.P., Lim, S.G., Hong, W., 2005b. The severe acute respiratory syndrome coronavirus 3a protein up-regulates expression of fibrinogen in lung epithelial cells. J. Virol. 79, 10083–10087.

Thomson, B.J., 2001. Viruses and apoptosis. Int. J. Exp. Pathol. 82, 65–76.

Xu, J., Zhong, S., Liu, J., Li, L., Li, Y., Wu, X., Li, Z., Deng, P., Zhang, J., Zhong, N., Ding, Y., Jiang, Y., 2005. Detection of severe acute respiratory syndrome coronavirus in the brain: potential role of the chemokine mig in pathogenesis. Clin. Infect. Dis. 41, 1089–1096.

Yan, H., Xiao, G., Zhang, J., Hu, Y., Yuan, F., Cole, D.K., Zheng, C., Gao, G.F., 2004. SARS coronavirus induces apoptosis in Vero E6 cells. J. Med. Virol. 73, 323–331.

Yount, B., Roberts, R.S., Sims, A.C., Deming, D., Frieman, M.B., Sparks, J., Denison, M.R., Davis, N., Baric, R.S., 2005. Severe acute respiratory syndrome coronavirus group-specific open reading frames encode nonessential functions for replication in cell cultures and mice. J. Virol. 79, 14909–14922.

Yu, C.-J., Chen, Y.-C., Hsiao, C.-H., Kuo, T.-C., Chang, S.C., Lu, C.-Y., Wei, W.-C., Lee, C.-H., Huang, L.-M., Chang, M.-F., Ho, H.-N., Lee, F.-J.S., 2004. Identification of a novel protein 3a from severe acute respiratory syndrome coronavirus. FEBS Lett. 565, 111–116.

Yuan, X., Shan, Y., Zhao, Z., Chen, J., Cong, Y., 2005a. G0/G1 arrest and apoptosis induced by SARS-CoV 3b protein in transfected cells. Virol. J. 2, 66.

Yuan, X., Yao, Z., Shan, Y., Chen, B., Yang, Z., Wu, J., Zhao, Z., Chen, J., Cong, Y., 2005b. Nucleolar localization of non-structural protein 3b, a protein specifically encoded by the severe acute respiratory syndrome coronavirus. Virus Res. 114, 70–79.

Zeng, R., Yang, R.F., Shi, M.D., Jiang, M.R., Xie, Y.H., Ruan, H.Q., Jiang, X.S., Shi, L., Zhou, H., Zhang, L., Wu, X.D., Lin, Y., Ji, Y.Y., Xiong, L., Jin, Y., Dai, E.H., Wang, X.Y., Si, B.Y., Wang, J., Wang, H.X., Wang, C.E., Gan, Y.H., Li, Y.C., Cao, J.T., Zuo, J.P., Shan, S.F., Xie, E., Chen, S.H., Jiang, Z.Q., Zhang, X., Wang, Y., Pei, G., Sun, B., Wu, J.R., 2004. Characterization of the 3a protein of SARS-associated coronavirus in infected vero E6 cells and SARS patients. J. Mol. Biol. 341, 271–279.

Zhivotosky, B., 2004. Apoptosis, necrosis and between. Cell Cycle 3, 64–66.